Some Tools for Adaptivity in the Spectral Element Method

M. Azaïez* C.Bernardi† Y. Maday†‡

Abstract

Mesh adaptivity in the spectral element framework consists either in refining the decomposition into subdomains or in increasing the degree of the polynomials, so its numerical analysis relies on the $h-N$ version of the method. Two different tools for adaptivity are presented and studied: error indicators and decomposition by the mortar technique. Some numerical experiments are given.

Key words: spectral elements, adaptivity, domain decomposition.

AMS subject classifications: 65N30, 65N35, 65N55.

1 Introduction

Mesh adaptivity has become an essential tool in the framework of finite element methods since it plays an important role for the efficiency of the discretization and the reliability of the numerical results. The aim of this paper is to present a tentative extension to the spectral element method. This one consists in approximating the solution of a partial differential equation by functions which are high degree polynomials on each rectangle of a nonoverlapping decomposition of the initial domain, by using tensorized polynomial bases that are associated with tensorized Gauss-type formulas.

From this description, it can easily be seen that the spectral element mesh is constructed on two levels: the domain decomposition and the choice of the quadrature formula on each rectangle since its nodes form the grid on this rectangle. So, two levels of adaptivity exist: the *decomposition adaptivity* consists in cutting up the initial rectangles, the *degree adaptivity* in increasing the degree of the polynomials on a fixed rectangle, resulting in a refinement of the local grid.

With the two levels, we associate two parameters: the first one, denoted by h, represents the lengths of the largest edge of each rectangle, the second one, denoted by N, is the set of the maximal degrees of polynomials inside each rectangle. So, we are led to work with the so-called $h-N$ version of the spectral element method.

We work with the model problem of a Laplace equation with homogeneous Dirichlet boundary conditions. As a first tool, we describe several families of error indicators which should allow for an efficient refinement of the decomposition and an optimized choice of the degree. We recall the concluding results of their numerical analysis which is performed in [2], in one and two dimensions. As a second tool, we propose a way of working on the cut up rectangles, even if the new mesh is not conforming, by the mortar element method in $h-N$ version, in analogy to the study of [5] for finite elements. Some numerical results are given, for the error indicators in order to compare them with the local error between the exact and discrete solutions and for the domain adaptivity in order to check its efficiency.

An outline of the paper is as follows. In Section 2, we make some basic assumptions on the initial decomposition of the domain, and we introduce the exact and discrete problems. In Section 3, we describe the error indicators and present some numerical experiments. Section 4 is devoted to decomposition adaptivity by the mortar method. The results of a first numerical test about adaptivity are given in Section 5. In Section 6, we propose some possible extensions of our analysis.

*Laboratoire de Modélisation en Mécanique des Fluides, Université Paul Sabatier, F–31062 Toulouse Cedex, France.

†Analyse Numérique, C.N.R.S. & Université Pierre et Marie Curie, B.C. 187, 4 place Jussieu, F-75252 Paris Cedex 05, France.

‡Laboratoire ASCI, Batiment 506 University Paris Sud, 91405 ORSAY cedex, France

ICOSAHOM'95: Proceedings of the Third International Conference on Spectral and High Order Methods.

2 The geometry and the model problem.

Let Ω be a bounded open polygon in $\mathbb{R}^2$ (sometimes a bounded open interval in $\mathbb{R}$). From now on, we assume that it admits a family of decompositions into disjoint rectangles (intervals), only for the sake of simplicity since most results extend to straight or curved quadrilaterals. More precisely, there exists a finite number of open rectangles (intervals) Ω_k, $1 \le k \le K$, such that

$$(1) \qquad \overline{\Omega} = \bigcup_{k=1}^{K} \overline{\Omega}_k \qquad \text{and} \qquad \Omega_k \cap \Omega_\ell = \emptyset, \quad k \ne \ell.$$

The decomposition is characterized by a K-tuple $h = (h_k)_{1 \le k \le K}$, where h_k is the length of the largest edge of Ω_k. In the two-dimensional case, we choose to make the following hypotheses on this decomposition, although more technical arguments would allow to avoid them.

Conformity hypothesis: The intersection of $\overline{\Omega}_k$ and $\overline{\Omega}_\ell$, $1 \le k \ne \ell \le K$, is either empty or a corner or an edge of both $\overline{\Omega}_k$ and $\overline{\Omega}_\ell$.

First regularity hypothesis: The ratio of the length of the largest edge of each Ω_k to the length of the smallest one is bounded independently of k and of the decomposition, i.e. of h.

On the domain Ω and on each subdomain, we use the standard notation for the Hilbertian Sobolev spaces, their usual norms and seminorms.

In this paper, we limit ourselves to the model problem

$$(2) \qquad \begin{cases} -\Delta u = f & \text{in } \Omega, \\ u = 0 & \text{on } \partial\Omega. \end{cases}$$

In view of the discretization, the function f is supposed to be continuous on $\overline{\Omega}$.

Next, in order to define the discrete problem, we introduce on each Ω_k and for a positive integer N_k the space $\mathbb{P}_{N_k}(\Omega_k)$ of restrictions to Ω_k of all polynomials of degree $\le N_k$ with respect to each variable. In the two-dimensional case, we make the last hypothesis (which can be skipped out, see [2] for the details).

Second regularity hypothesis: The ratio N_k/N_ℓ for all pairs of rectangles Ω_k and Ω_ℓ that share one edge is bounded independently of k and ℓ and of the decomposition, i.e. of h.

Denoting by N the K-tuple $(N_k)_{1 \le k \le K}$, we are going to work with the global parameter (h, N). And we introduce the discrete spaces

$$Z_{hN} = \Big\{ v_{hN} \in L^2(\Omega);\ v_{hN\,|\Omega_k} \in \mathbb{P}_{N_k}(\Omega_k),\ 1 \le k \le K \Big\},$$
$$(3) \qquad X_{hN} = Z_{hN} \cap H_0^1(\Omega).$$

Note that the functions of X_{hN} are continuous. In all that follows, c stands for a generic constant independent of h and N.

Finally, on the open reference interval $]-1, 1[$, we introduce the nodes ξ_j and the weights ρ_j, $0 \le j \le n$, of the standard Gauss–Lobatto formula which is exact on all polynomials with degree $\le 2n - 1$. Taking n equal to N_k allows for defining by affine transformation and tensorization the corresponding nodes $\boldsymbol{x}_{ij}^k$ and weights ρ_{ij}^k, $0 \le i, j \le N_k$, on each domain Ω_k (forget the index j in the one-dimensional case). This leads to the discrete product, for all continuous functions v and w on $\overline{\Omega}$:

$$(4) \qquad (v, w)_{hN} = \sum_{k=1}^{K} \sum_{i=0}^{N_k} \sum_{j=0}^{N_k} v(\boldsymbol{x}_{ij}^k)\, w(\boldsymbol{x}_{ij}^k)\, \rho_{ij}^k.$$

We also denote by $\mathcal{I}_{hN}$ the usual Lagrange interpolation operator at these nodes, with values in Z_{hN}.

Now, the discrete problem reads: *find u_{hN} in X_{hN} such that*

$$(5) \qquad (\mathbf{grad}\, u_{hN}, \mathbf{grad}\, v_{hN})_{hN} = (f, v_{hN})_{hN}, \qquad \forall v_{hN} \in X_{hN}.$$

The positivity property of the Gauss–Lobatto quadrature formula (see [4, Rem. 13.3]) yields that it has a unique solution u_{hN}. And using the standard spectral arguments on a reference square leads to the

A priori estimate: There exists a positive constant c independent of h and N such that, if the solution u (resp. the function f) of problem (2) is such that $u_{|\Omega_k}$ (resp. $f_{|\Omega_k}$) belongs to $H^{s_k}(\Omega_k)$, $s_k \ge 1$ (resp. to $H^{\sigma_k}(\Omega_k)$, $\sigma_k > 1$) for $1 \le k \le K$, the following estimate holds between u and the solution u_{hN} of problem (5):

$$(6) \qquad \|u - u_{hN}\|_{H^1(\Omega)} \le c \sum_{k=1}^{K} \Big(h_k^{\inf\{s_k - 1, N_k\}} N_k^{1 - s_k} \|u\|_{H^{s_k}(\Omega_k)} + h_k^{\inf\{\sigma_k, N_k + 1\}} N_k^{-\sigma_k} \|f\|_{H^{\sigma_k}(\Omega_k)} \Big).$$

3 Error indicators.

On the present decomposition of the domain, a family of error indicators will be a K-tuple $(\eta_k)_{1 \le k \le K}$ satisfying for some positive constants κ_{1hN} and κ_{2hN},

$$(7) \quad |u - u_{hN}|_{H^1(\Omega)} \leq \kappa_{1hN} \Big(\sum_{k=1}^{K} \eta_k^2\Big)^{\frac{1}{2}} + c\,\|f - \mathcal{I}_{hN} f\|_{L^2(\Omega)},$$

$$(8) \quad \eta_k \leq \kappa_{2hN}\, |u - u_{hN}|_{H^1(\omega_k)} + c\,\|f - \mathcal{I}_{hN} f\|_{L^2(\omega_k)}, 1 \leq k \leq K,$$

where ω_k stands for the union of the Ω_ℓ which share at least an edge (an endpoint in the one-dimensional case) with Ω_k and c is independent of h and N.

A family of error indicators is said to be optimal if both constants κ_{1hN} and κ_{2hN} are bounded independently of h and N. For the indicators that we present here, the optimality is proven in the one-dimensional case but not in higher dimensions.

The following indicators are derived from analogous residual type indicators in the finite element method, see [8] and [9] for instance, however weights are introduced in order to improve the optimality, more precisely to obtain better bounds for κ_{1hN} and κ_{2hN} (in the one-dimensional case, the results would not be optimal without weight). We refer to [2] for the proof of the estimates stated below.

One-dimensional indicators: Here, we set

$$(9) \qquad \eta_k = N_k^{-1}\, \|(\mathcal{I}_{hN} f + u''_{hN})\, d_k^{\frac{1}{2}}\|_{L^2(\Omega_k)},$$

where d_k stands for the product of the distances to both endpoints of Ω_k.

With definition (9), estimates (7) and (8) hold with constants κ_{1hN} and κ_{2hN} independent of h and N (more precisely with $\kappa_{1hN} = 1$ and $\kappa_{2hN} = \sqrt{6}$ for instance).

Note however that, in the one-dimensional case, the regularity of the solution u only depends on the function f; as a consequence, the leading error in (7) and (8) comes from the term $f - \mathcal{I}_{hN} f = -u'' + \mathcal{I}_{hN}(u'')$. So, to verify numerically the independence of the constants κ_{1hN} and κ_{2hN} with respect to the discretization parameters, we have to make this contribution negligible. This is done by using the following modifications: solving problem (5) with the discrete product replaced by $(.,.)_{hM}$ and computing the η_k by (9) with the interpolate term $\mathcal{I}_{hN} f$ replaced by $\mathcal{I}_{hM} f$, where M is a K-tuple of integers M_k larger than N_k.

Bidimensional indicators: Let us denote by $\Gamma_{k,\ell}$, $1 \leq \ell \leq L(k)$, the edges of Ω_k which are not contained in $\partial\Omega$. Introducing a parameter α, $0 \leq \alpha \leq 1$, we set

$$(10) \quad \eta_k^\alpha = h_k^{1-2\alpha}\, N_k^{-1}\, \|(\mathcal{I}_{hN} f + \Delta u_{hN})\, d_k^{\frac{\alpha}{2}}\|_{L^2(\Omega_k)} + \frac{1}{2} h_k^{\frac{1}{2}-\alpha}\, N_k^{-\sup\{\frac{1}{2},\alpha\}} \sum_{\ell=1}^{L(k)} \|[\partial_n u_{hN}]\, d_{k,\ell}^{\frac{\alpha}{2}}\|_{L^2(\Gamma_{k,\ell})},$$

where d_k is now the product of the distances to the four edges of Ω_k and $d_{k,\ell}$ stands for the product of the distances to both endpoints of $\Gamma_{k,\ell}$. Clearly, $[\partial_n u_{hN}]$ denotes the jump of the normal derivative of the discrete solution u_{hN} through each $\Gamma_{k,\ell}$. We only state the results for the basic cases $\alpha = 0$, $\alpha = \frac{1}{2}$ and $\alpha = 1$, we refer to [2] for their extension to general values of α between 0 and 1.

Let $\bar{N}$ stand for the maximum of the N_k, $1 \leq k \leq K$. Let also ε be any positive real number. For $\alpha = 0$, with the further assumption that the product $h_k N_k (\log N_k)^{-\frac{3}{2}}$ for any $\overline{\Omega}_k$ that contains a re-entrant corner of Ω is larger than a constant independent of h and N, estimates (7) and (8) hold with

$$(11) \qquad \kappa_{1hN} \leq c \quad \text{and} \quad \kappa_{2hN} \leq c\, \bar{N}^{\frac{3}{2}+\varepsilon}.$$

For $\alpha = \frac{1}{2}$, estimates (7) and (8) hold with

$$(12) \qquad \kappa_{1hN} \leq c\, \bar{N}^{\frac{1}{4}+\varepsilon} \quad \text{and} \quad \kappa_{2hN} \leq c\, \bar{N}^{\frac{1}{2}+\varepsilon}.$$

For $\alpha = 1$, estimates (7) and (8) hold with

$$(13) \qquad \kappa_{1hN} \leq c\, \bar{N}^{\frac{5}{4}+\varepsilon} \quad \text{and} \quad \kappa_{2hN} \leq c.$$

It can be noted that these constants are always independent of h (this allows for proving that the indicators defined in (10) are optimal for quadrilateral finite elements on a structured mesh), but they depend on N. However, the product $\kappa_{1hN}\kappa_{2hN}$ is always smaller than $\bar{N}^{\frac{3}{2}+\varepsilon}$. Also, the first inequality in (11) which is optimal allows for computing an explicit upper bound for the error.

We present some numerical experiments in order to test and compare the previous indicators, firstly in the case of one subdomain in one or two dimensions: then, the index k is skipped over and the discretization parameter is the maximal degree N of the polynomials in this domain. For already explained reasons, we replace N by $M = 48 \times 48$ in the right-hand side of problem (5) and in the interpolate of the function f in definition (9) or (10).

Each of the four following figures represent, in logarithmic scale, the "exact" error $E = |u - u_{hN}|_{H^1(\Omega)}$ (evaluated by replacing u by $\mathcal{I}_N u$) and the indicator η in the one-dimensional case, the three indicators η^0, $\eta^{\frac{1}{2}}$ and η^1 in the two-dimensional case, as a function of N for $8 \leq N \leq 64$.

In Figure 1 and Figure 2, the domain Ω is $]-1, 1[$, and the two solutions u are respectively

$$u_1(x) = (1 - x^2)^{\frac{5}{2}}, \qquad u_2(x) = (1 - x^2)^{\frac{9}{4}}.$$

The theoretical slopes for the exact error E, given by the usual arguments of polynomial approximation (see [4, Rem. 6.4]), are respectively - 4 and - 3.5. The numerical

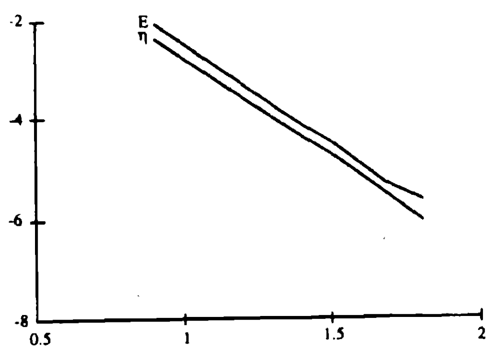

Figure 1

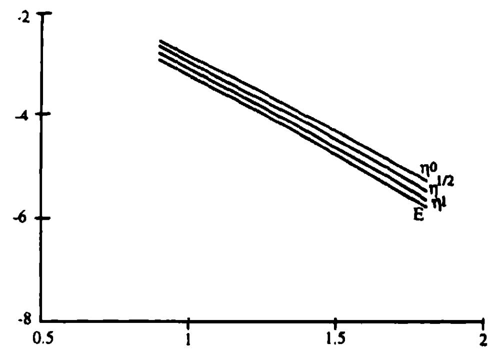

Figure 3

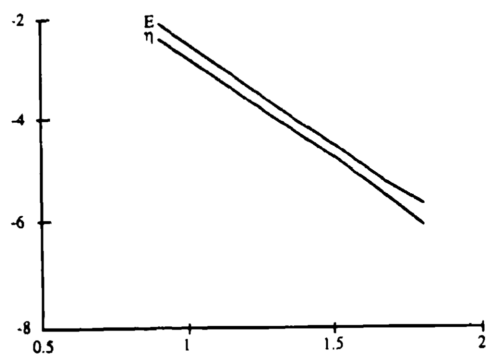

Figure 2

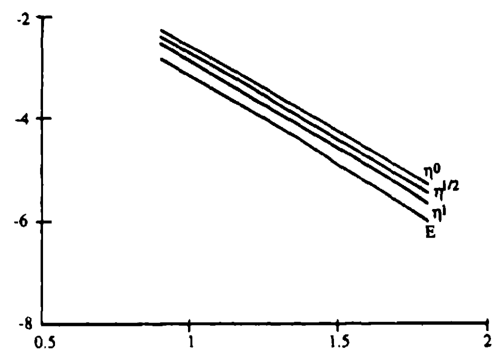

Figure 4

slopes for the error are respectively - 4.05 and - 3.42, the slopes for the indicators are respectively - 3.94 and - 3.49.

In Figure 3 and Figure 4, the domain Ω is $]-1,1[^2$, and the two solutions u are respectively

$$u_3(x,y) = (1-x^2)^{\frac{5}{2}}\,(1-y^2)^{\frac{5}{2}},$$

$$u_4(x,y) = (1-x^2)^{\frac{9}{4}}\,(1-y^2)^{\frac{9}{4}}.$$

The slopes are given in Table 1.

In Figure 5, the domain Ω is now $]-1,3[\times]-1,1[$, with the decomposition into $\Omega_1 =]-1,1[\times]-1,1[$ and $\Omega_2 =]1,3[\times]-1,1[$, and the solution u is given by

$$u(x,y) = (1+x)^{\frac{5}{2}}\,(3-x)^3\,(1-y^2)^3,$$

so it is less regular in the left subdomain than in the right one. The following figure represents, in logarithmic scales, the local errors $E_k = |u-u_{hN}|_{H^1(\Omega_k)}$ and the three indicators η_k^0, $\eta_k^{\frac{1}{2}}$ and η_k^1 for $k=1$ and 2.

The results are in good coherency with estimates (11) to (13), up to a multiplicative constant on the indicators. In particular, in Figure 5, the indicators clearly show the lack of regularity of the solution on the left subdomain. Comparing the indicators and their slopes to the exact error and its slope would lead to choose $\alpha = 1$, however the difference between the three indicators is relatively small.

Degree adaptivity: In the definition of the η_k^α, the term $\mathcal{I}_{hN} f + \Delta u_{hN}$ can be expanded in the tensorized basis of Jacobi polynomials that are orthogonal for the measure $d_k^\alpha(x,y)\,dx\,dy$: the Legendre polynomials for $\alpha = 0$, the Chebyshev polynomials of the second kind for $\alpha = \frac{1}{2}$, the derivatives of the Legendre polynomials for $\alpha = 1$. Of course, each coefficient of the expansion can be evaluated by an appropriate quadrature formula.

This leads to insert the equality

$$\eta_k^\alpha = \Big(\sum_{m=1}^{N}\sum_{n=1}^{N}(\eta_{kmn}^\alpha)^2\Big)^{\frac{1}{2}}$$

in (7). Conversely, it can be proven that each η_{kmn}^α is bounded by a combination of the coefficients of order

	E (theor.)	E (numer.)	η^0	$\eta^{\frac{1}{2}}$	η^1
Function u_3	-4	-3.52	-3.35	-3.44	-3.48
Function u_4	-3.5	-3.18	-3.06	-3.13	-3.16

Table 1:

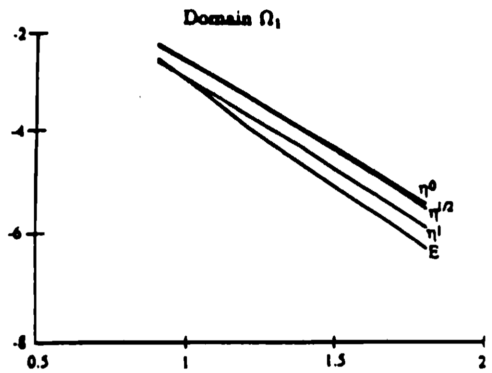

Figure 5.1

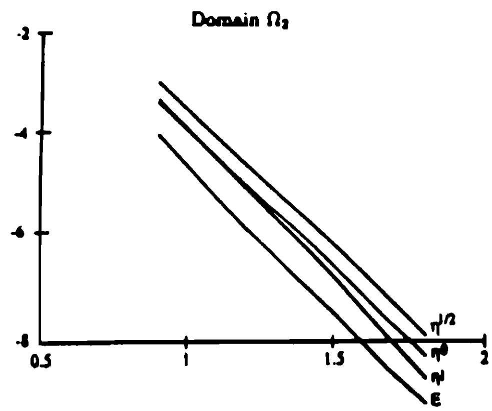

Figure 5.2

(m, n) and $(m \pm 1, n \pm 1)$ of the error $\mathbf{grad}\,(u - u_{hN})$ on Ω_k in an orthogonal basis, in the same spirit as (8). Then, the general algorithm for adaptivity could be:

- computing the η_k^α;
- for each k such that η_k^α is large, computing some η_{kmn}^α;
- if the η_{kmn}^α for large values of $m+n$ are small or decrease with $m+n$, cutting up the element Ω_k; if not, increasing the maximal degree N_k.

4 Decomposition by the mortar technique.

In the two-dimensional case, cutting up the rectangles into subrectangles in adequation with the previously computed error indicators is very easy, however preserving the conformity property (as stated in the conformity hypothesis) could lead to highly increasing the number of degrees of freedom in the new discrete problem. The following Figure 6 presents a basic example, where only the three rectangles containing the re-entrant corner have to be cut up into four subrectangles for adaptivity but six further rectangles have to be cut up in two for conformity reasons.

However, the mortar element method [6, 7] is known for efficiently handling the nonconforming decomposition and was used in [5] to treat nonconforming refinements in the finite element case, we now describe the analogous procedure for the spectral element method. So, let us assume that, among the rectangles Ω_k, $1 \le k \le K$, only the K^* first ones Ω_1, Ω_2, ... and Ω_{K^*} must be cut up into m^2 open subrectangles $\Omega_{kk'}$, $1 \le k' \le m^2$ (only for the sake of brevity, we take the same m for all rectangles). We define the open subdomains Δ_m and Δ_1 by

$$(14)\quad \overline{\Delta}_m = \bigcup_{k=1}^{K^*} \overline{\Omega}_k = \bigcup_{k=1}^{K^*} \bigcup_{k'=1}^{m^2} \overline{\Omega}_{kk'}, \qquad \Delta_1 = \Omega \setminus \overline{\Delta}_m.$$

We introduce new integers $N_k^* \ge N_k$, $K^* + 1 \le k \le K$, and $N_{kk'} \ge N_k$, $1 \le k \le K^*$ and $1 \le k' \le m^2$, in order to take into account the possible degree adaptivity. On Δ_1, the discrete functions are restrictions of continuous

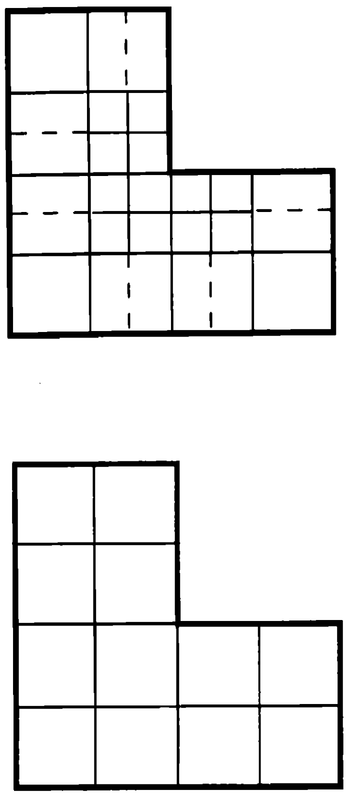

Figure 6

functions in Z_{hN} for a modified value of N:

$$X_{hN}(\Delta_1) =$$

$$\Big\{v_{hN} \in C^0(\overline{\Delta}_1);\ v_{hN\,|\Omega_k} \in \mathbb{P}_{N_k^*}(\Omega_k),\ K^*+1 \le k \le K\Big\},$$

while on Δ_m they now are polynomials on the subrectangles:

$$X_{hN}(\Delta_m) = \Big\{v_{hN} \in C^0(\overline{\Delta}_m);\ v_{hN\,|\Omega_{kk'}} \in \mathbb{P}_{N_{kk'}}(\Omega_{kk'}),\ 1 \le k \le K^*,\ 1 \le k' \le m^2\Big\}.$$

Next, let Γ_ℓ, $1 \le \ell \le L$, denote the edges of the Ω_k, $K^*+1 \le k \le K$, that are contained in $\partial\Delta_1 \cap \partial\Delta_m$. Each Γ_ℓ is the edge of two rectangles $\Omega_{k_1(\ell)}$ and $\Omega_{k_m(\ell)}$, with $K^*+1 \le k_1(\ell) \le K$ and $1 \le k_m(\ell) \le K^*$. Thus, on this edge, we define a trace subspace $W_{hN}(\Gamma_\ell)$ in one of the two following ways:
– in the first case, $W_{hN}(\Gamma_\ell)$ coincides with $\mathbb{P}_{N_{k_1(\ell)}-2}(\Gamma_\ell)$ (which is a subspace of traces on Γ_ℓ of functions in $X_{hN}(\Delta_1)$); then Γ_ℓ is said to be of type 1;
– in the second case, $W_{hN}(\Gamma_\ell)$ is the subspace of traces on Γ_ℓ of functions in $X_{hN}(\Delta_m)$, made of functions that are polynomial with degree $N_{kk'}-1$ on the edges of the two $\Omega_{kk'}$ which contain the endpoints of Γ_ℓ, with $k = k_m(\ell)$; then, Γ_ℓ is said to be of type m.

Finally, the mortar discrete space X^*_{hN} is defined as the space of all functions v_{hN} satisfying:
(i) $v_{hN\,|\Delta_1}$ belongs to $X_{hN}(\Delta_1)$ and $v_{hN\,|\Delta_m}$ belongs to $X_{hN}(\Delta_m)$,
(ii) v_{hN} vanishes on $\partial\Omega$,
(iii) there exists a function φ, called mortar function, such that
– on all Γ_ℓ of type 1, φ coincides with the trace of $v_{hN|\Delta_m}$ and

$$(15)\quad \int_{\Gamma_\ell} (v_{hN|\Delta_1} - \varphi)(\tau)\psi(\tau)\,d\tau = 0,\ \forall\psi \in W_{hN}(\Gamma_\ell)$$

– on all Γ_ℓ of type m, φ coincides with the trace of $v_{hN|\Delta_1}$ and

$$(16)\quad \int_{\Gamma_\ell} (v_{hN|\Delta_m} - \varphi)(\tau)\psi(\tau)\,d\tau = 0,\ \forall\psi \in W_{hN}(\Gamma_\ell).$$

It can be noted that the space X^*_{hN} is never contained in $H^1_0(\Omega)$, so the discretization is nonconforming.

With obvious extensions of the notation for nodes and weights, the new discrete product is now defined, for all continuous functions v and w on $\overline{\Omega}$, by:

$$(17)\quad (v,w)^*_{hN} = \sum_{k=K^*+1}^{K} \sum_{i=0}^{N_k^*} \sum_{j=0}^{N_k^*} v(\boldsymbol{x}_{ij}^{k*})\,w(\boldsymbol{x}_{ij}^{k*})\,\rho_{ij}^{k*} + \sum_{k=1}^{K^*} \sum_{k'=1}^{m^2} \sum_{i=0}^{N_{kk'}} \sum_{j=0}^{N_{kk'}} v(\boldsymbol{x}_{ij}^{kk'})\,w(\boldsymbol{x}_{ij}^{kk'})\,\rho_{ij}^{kk'}.$$

And the new discrete problem reads: *find u^*_{hN} in X^*_{hN} such that*

$$(18)\quad (\mathbf{grad}\, u^*_{hN}, \mathbf{grad}\, v_{hN})^*_{hN} = (f, v_{hN})^*_{hN},\quad \forall v_{hN} \in X^*_{hN}.$$

The end of this section is devoted to the numerical analysis of problem (18), in order to prove that it has the same properties as problem (5) in spite of its nonconformity.

Wellposedness: Problem (18) can equivalently be written as a linear system with as many unknowns as equations, so we only have to check that for null data its only solution is 0. This is a consequence of the following argument: if $(\mathbf{grad}\, u^*_{hN}, \mathbf{grad}\, u^*_{hN})^*_{hN}$ is 0, the positivity of the quadrature formulas implies that $\mathbf{grad}\, u^*_{hN}$ is 0, so that u^*_{hN} is a constant on each subdomain Δ_1 and Δ_m where it is continuous. Then, the matching conditions (15) and (16) are sufficient to enforce that the two constants are equal and, thanks to the boundary conditions on u^*_{hN}, they are 0. Hence, problem (18) has a unique solution.

Next, in order to work with discontinuous functions in X^*_{hN}, we introduce the broken seminorm and norm on Ω:

$$(19)\qquad |v|_{1*} = \left(|v|^2_{H^1(\Delta_1)} + |v|^2_{H^1(\Delta_m)}\right)^{\frac{1}{2}}$$
$$\text{and}\quad \|v\|_{1*} = \left(\|v\|^2_{H^1(\Delta_1)} + \|v\|^2_{H^1(\Delta_m)}\right)^{\frac{1}{2}}.$$

From the previous lines, we derive that there exists a positive constant α_{hN}, possibly depending on h and N, such that the following ellipticity property holds:

$$(20)\quad (\mathbf{grad}\, v_{hN}, \mathbf{grad}\, v_{hN})^*_{hN} \geq \alpha_{hN}\, \|v_{hN}\|^2_{1*}, \quad \forall v_{hN} \in X^*_{hN}.$$

Then, the following estimate holds for any function v_{hN} in X^*_{hN} and any function f_{hN} which are polynomial of degree $\leq N^*_k - 1$ on each Ω_k, $K^* + 1 \leq k \leq K$, and of degree $\leq N_{kk'} - 1$ on each $\Omega_{kk'}$, $1 \leq k \leq K^*$, $1 \leq k' \leq m^2$:

$$(21)\quad \|u - u^*_{hN}\|_{1*} \leq c\,(1 + \alpha^{-1}_{hN}) \Big(\|u - v_{hN}\|_{1*} + \sup_{w_{hN} \in X^*_{hN}} \frac{\sum_{\ell=1}^{L} \int_{\Gamma_\ell} (\partial_n u)(\tau)[w_{hN}](\tau)\, d\tau}{\|w_{hN}\|_{1*}} + \|f - f_{hN}\|_{L^2(\Omega)} + \|f - \mathcal{I}^*_{hN} f\|_{L^2(\Omega)}\Big),$$

where $\mathcal{I}^*_{hN}$ stands for the Lagrange interpolation operator on the new mesh. The last term being evaluated from standard arguments [4, § 7 and § 14], we only study the behavior of the ellipticity constant α_{hN} and we briefly explain the analysis of the approximation error and consistency error that appear in the right-hand side.

Uniform ellipticity: Here, we prove the following basic property: there exists a constant β independent of h and N such that

$$(22)\qquad \|v_{hN}\|_{L^2(\Omega)} \leq \beta\, |v_{hN}|_{1*},\ \forall v_{hN} \in X^*_{hN}.$$

Indeed, it can be assumed without restriction that Ω is a rectangle $]a, a'[\times]b, b'[$ (since both the mesh and functions in X^*_{hN} can obviously be extended to a larger rectangle). The line of fixed coordinate y crosses $\partial\Delta_1 \cap \partial\Delta_m$ at a finite number of points of edges $\Gamma_{\ell,i}$, denoted by (a^y_i, y), $1 \leq i \leq I$, in increasing order of x coordinate. So, we can write (with $a^y_i < x \leq a^y_{i+1}$)

$$v_{hN}(x, y) = \int_a^{a^y_1} (\partial_x v_{hN})(t, y)\, dt + [v_{hN}(a^y_1, y)] + \int_{a^y_1}^{a^y_2} (\partial_x v_{hN})(t, y)\, dt + \cdots + \int_{a^y_i}^{x} (\partial_x v_{hN})(t, y)\, dt.$$

Next, we integrate on Ω the square of this equation: with $a^y_0 = a$ and $a^y_{I+1} = a'$,

$$\|v_{hN}\|^2_{L^2(\Omega)} \leq 2 \int_\Omega \Big(\sum_{i=1}^{I+1} \int_{a^y_{i-1}}^{a^y_i} (\partial_x v_{hN})(t, y)\, dt\Big)^2\, dx\, dy + 2 \int_\Omega \Big(\sum_{i=1}^{I} [v_{hN}(a^y_i, y)]\Big)^2\, dx\, dy$$

Using Cauchy–Schwarz inequalities leads to

$$\|v_{hN}\|^2_{L^2(\Omega)} \leq 2(a' - a)^2 \left(\|\partial_x v_{hN}\|^2_{L^2(\Delta_1)} + \|\partial_x v_{hN}\|^2_{L^2(\Delta_m)}\right) + 2(a' - a) \int_b^{b'} \Big(\sum_{i=1}^{I} h_{\ell,i}\Big) \Big(\sum_{i=1}^{I} h^{-1}_{\ell,i}\, [v_{hN}(a^y_1, y)]^2\Big)\, dy),$$

where $h_{\ell,i}$ is the length of $\Gamma_{\ell,i}$. From the first regularity hypothesis, we observe that the length of the rectangle with edge $\Gamma_{\ell,i}$ in Δ_1 is bounded by c times its width, so that

$$\sum_{i=1}^{I} h_{\ell,i} \leq c\,(a' - a).$$

On the other hand, it follows from the orthogonality of the jump $[v_{hN}]$ to the constants in $L^2(\Gamma_{\ell,i})$ that

$$h^{-1}_\ell \int_{\Gamma_\ell} [v_{hN}(\tau)]^2\, d\tau \leq c\, \|[v_{hN}]\|^2_{H^{\frac{1}{2}}_{00}(\Gamma_\ell)} \leq c' \left(\|v_{hN}\|^2_{H^1(\Omega_{k_1(\ell)})} + \|v_{hN}\|^2_{H^1(\Omega_{k_m(\ell)})}\right).$$

Inserting these estimates in the previous lines implies (22) with β only depending on the first regularity hypothesis and the diameter of Ω.

As a consequence of (22), the ellipticity constant α_{hN} can be chosen independent of h and N.

Approximation error: As detailed in [6], the construction relies on the following result [3, Thm 3.g.10]: there exists a lifting operator R_n which associates with a polynomial φ_n in $\mathbb{P}_n(-1, 1)$ which vanishes at ± 1, a polynomial in $\mathbb{P}_n(]-1, 1[^2)$ such that its trace is equal to φ_n on one edge of the square, to 0 on the three other edges and such that its norm in $H^1(]-1, 1[^2)$ is bounded by a constant (independent of n) times $\|\varphi_n\|_{H^{\frac{1}{2}}_{00}(-1,1)}$. So the idea for exhibiting a function in X^*_{hN} which approximates the solution u is: starting from the interpolate $\mathcal{I}^*_{hN}u$, next lifting the jumps at the nonconforming points of $\partial\Delta_1 \cap \partial\Delta_m$ by multiplying them by a low degree function, and finally lifting the jumps through the edges thanks to the previous operator transported on each rectangle and subrectangle.

Consistency error: From conditions (15) and (16) together with the definition of φ, it can be observed that

$$\int_{\Gamma_\ell} (\partial_n u)(\tau)[w_{hN}](\tau)\,d\tau$$

$$\leq \int_{\Gamma_\ell} (\partial_n u - \pi_{hN,\ell}\partial_n u)(\tau)[w_{hN}](\tau)\,d\tau$$

$$\leq \|\partial_n u - \pi_{hN,\ell}\partial_n u\|_{(H^{\frac{1}{2}}(\Gamma_\ell))'}$$

$$\left(\|w_{hN}\|_{H^1(\Omega_{k_1(\ell)})} + \|w_{hN}\|_{H^1(\Omega_{k_m(\ell)})}\right),$$

where $\pi_{hN,\ell}$ is the orthogonal projection operator from $L^2(\Gamma_\ell)$ onto $W_{hN}(\Gamma_\ell)$. So the desired estimates follow from the properties of the analogous projection operator in $L^2(-1,1)$, see [6, Lemma 2.1].

Inserting all these results in (21), we derive the final estimates: if the solution u (resp. the function f) of problem (2) is such that its restriction to Ω_k belongs to $H^{s_k}(\Omega_k)$, $s_k > \frac{3}{2}$ (resp. to $H^{\sigma_k}(\Omega_k)$, $\sigma_k > 1$) for $K^*+1 \leq k \leq K$ and its restriction to $\Omega_{kk'}$ belongs to $H^{s_{kk'}}(\Omega_{kk'})$, $s_{kk'} > \frac{3}{2}$ (resp. to $H^{\sigma_{kk'}}(\Omega_{kk'})$, $\sigma_{kk'} > 1$) for $1 \leq k \leq K^*$, $1 \leq k' \leq m^2$, the following estimate holds between u and the solution u^*_{hN} of problem (18):

$$(23) \qquad \|u - u^*_{hN}\|_{1*}$$
$$\leq c \sum_{k=K^*+1}^{K} \Big(h_k^{\inf\{s_k-1,N_k\}} N_k^{*\,1-s_k} \|u\|_{H^{s_k}(\Omega_k)} + h_k^{\inf\{\sigma_k,N_k+1\}} N_k^{*\,-\sigma_k} \|f\|_{H^{\sigma_k}(\Omega_k)} \Big)$$
$$+c' \sum_{k=1}^{K^*} \sum_{k'=1}^{m^2} \Big(m^{-\inf\{s_{kk'}-1,N_{kk'}\}} h_k^{\inf\{s_{kk'}-1,N_{kk'}\}} N_{kk'}^{1-s_k} \|u\|_{H^{s_{kk'}}(\Omega_{kk'})} + m^{-\inf\{\sigma_{kk'},N_{kk'}+1\}} h_k^{\inf\{\sigma_{kk'},N_{kk'}+1\}} N_{kk'}^{-\sigma_{kk'}} \|f\|_{H^{\sigma_{kk'}}(\Omega_{kk'})} \Big).$$

This estimate is fully optimal with respect to any parameter but rather complicated. When all the h_k are equal to h and all the N^*_k, $N_{kk'}$ are equal to N, and if moreover the function f is assumed to be very regular and N is large enough, this estimate is easier to read: for any solution u such that $u_{|\Delta_1}$ belongs to $H^{s^*_1}(\Delta_1)$ and $u_{|\Delta_m}$ belongs to $H^{s^*_m}(\Delta_m)$,

$$(24) \qquad \|u - u^*_{hN}\|_{1*} \leq c\left(h^{s^*_1-1} N^{1-s^*_1} \|u\|_{H^{s^*_1}(\Delta_1)} + m^{1-s^*_m} h^{s^*_m-1} N^{1-s^*_m} \|u\|_{H^{s^*_m}(\Delta_m)}\right).$$

Moreover, let ε be any positive real number. Taking account of the corner singular functions leads to a modified estimate: if all the Ω_k containing a re-entrant corner of Ω are included in Δ_m as in Figure 6 (so that $\overline{\Delta_1}$ only contains convex corners),

$$\|u - u^*_{hN}\|_{1*} \leq c(f)\,(h^{2-\varepsilon} N^{\varepsilon-4} + m^{\varepsilon-\frac{2}{3}} h^{\frac{2}{3}-\varepsilon} N^{\varepsilon-\frac{4}{3}})$$

So, taking $m = h^{-2}N^4$ would optimize this estimate. This could be an argument for the choice of the initial mesh.

5 First experiment in adaptivity.

As a first test for the efficiency of the adaptivity, we present some numerical results in the one-dimensional case of the domain $\Omega =]0,1[$, when the solution u of problem (2) is

$$u(x) = x(1-x)\,|x - 0.065|^{\frac{9}{4}}.$$

Note that it is smooth except in the left part of the domain. Here, the function f is interpolated by $\mathcal{I}_{hN}f$ with the same N as for the discrete solution, so that the leading part of the error comes from this interpolation.

The first computation is performed on a decomposition of Ω in ten equal subdomains $\Omega_k =]\frac{k-1}{10}, \frac{k}{10}[$, $1 \leq k \leq 10$. Tables 2 and 3 present, for N equal to 16, 32, 64, the local errors $E_k = |u - u_{hN}|_{H^1(\Omega_k)}$ and the corresponding indicators η_k in the left five subdomains (the more interesting ones). Next, the discrete solution is computed with a decomposition of Ω in twenty equal subdomains $\tilde{\Omega}_\ell =]\frac{\ell-1}{20}, \frac{\ell}{20}[$, $1 \leq \ell \leq 20$. Table 4 presents, for N equal to 16, 32, 64, the errors E'_k on each Ω_k, $1 \leq k \leq 5$, computed as the square root of the sum of the $|u - u_{hN}|^2_{H^1(\tilde{\Omega}_\ell)}$ for the two $\tilde{\Omega}_\ell$ contained in Ω_k.

In a final step, the discrete solution is computed with a decomposition of Ω in twenty "adapted" subdomains which, according to the previous indicators, are chosen as follows: the first interval Ω_1 is divided into 11 equal elements, the other nine ones are left unchanged. Table 5 present, for N equal to 16, 32, 64, the errors E''_k on each Ω_k, $1 \leq k \leq 5$: the first one is the square root of the sum of the $|u - u_{hN}|^2_{H^1(\Omega_{1k'})}$ on the first eleven subdomains $\Omega_{1k'}$ contained in Ω_1, the other ones are the new error on the nonrefined intervals.

	E_1	E_2	E_3	E_4	E_5
$N = 16$	0.1×10^{-4}	0.9×10^{-6}	0.9×10^{-6}	0.9×10^{-6}	0.9×10^{-6}
$N = 32$	0.1×10^{-5}	0.9×10^{-7}	0.9×10^{-7}	0.9×10^{-7}	0.9×10^{-7}
$N = 64$	0.7×10^{-6}	0.9×10^{-7}	0.9×10^{-7}	0.9×10^{-7}	0.9×10^{-7}

Table 2:

	η_1	η_2	η_3	η_4	η_5
$N = 16$	0.4×10^{-5}	0.5×10^{-10}	0.3×10^{-10}	0.1×10^{-10}	0.6×10^{-11}
$N = 32$	0.9×10^{-6}	0.1×10^{-9}	0.2×10^{-9}	0.3×10^{-9}	0.2×10^{-9}
$N = 64$	0.4×10^{-6}	0.2×10^{-8}	0.3×10^{-8}	0.4×10^{-8}	0.7×10^{-8}

Table 3:

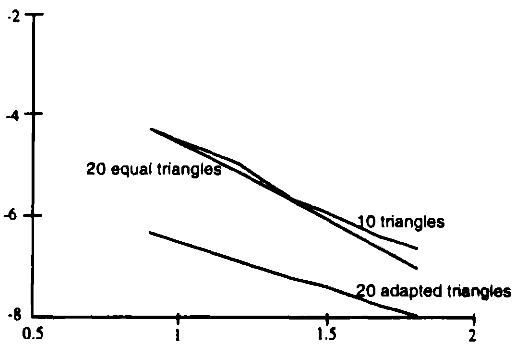

Figure 7

The efficiency of the adaptivity already appears in these tables. It can also be checked that the local refinement yields a small improvement of the error in all subdomains. In Figure 7, we present, in logarithmic scales and for N between 8 and 64, the global error $|u - u_{hN}|_{H^1(\Omega)}$ corresponding respectively to the ten equal intervals, to the twenty equal intervals and to the twenty adapted intervals.

6 Possible extensions.

In analogy to the finite element case [8, 9], it can be checked that the arguments for estimating the constants κ_{1hN} and κ_{2hN} hold for any elliptic problem of type: *find u in V such that*

$$\forall v \in V, \quad a(u, v) = \int_\Omega f(\boldsymbol{x}) v(\boldsymbol{x})\, d\boldsymbol{x},$$

for any polygonal domain Ω with angles $\frac{\pi}{2}$ and $\frac{3\pi}{2}$ and any closed subspace V of $L^2(\Omega)$ or $H^1(\Omega)$, when the bilinear form $a(\,.\,)$ is continuous and elliptic in V. Moreover, it also holds when this form satisfies an inf-sup condition of Babuška and Brezzi type: this is the case for the Stokes problem. So the estimates (11) to (13) should hold, with slight modifications, for any standard second-order problem with Dirichlet, Neumann or mixed boundary conditions.

	E_1'	E_2'	E_3'	E_4'	E_5'
$N = 16$	0.1×10^{-5}	0.1×10^{-6}	0.1×10^{-6}	0.1×10^{-6}	0.1×10^{-6}
$N = 32$	0.1×10^{-5}	0.7×10^{-7}	0.7×10^{-7}	0.7×10^{-7}	0.7×10^{-7}
$N = 64$	0.1×10^{-6}	0.1×10^{-7}	0.1×10^{-7}	0.1×10^{-7}	0.1×10^{-7}

Table 4:

	E_1''	E_2''	E_3''	E_4''	E_5''
$N = 16$	0.1×10^{-6}	0.2×10^{-7}	0.2×10^{-7}	0.2×10^{-7}	0.2×10^{-7}
$N = 32$	0.4×10^{-7}	0.5×10^{-8}	0.5×10^{-8}	0.5×10^{-8}	0.5×10^{-8}
$N = 64$	0.4×10^{-8}	0.8×10^{-9}	0.7×10^{-9}	0.1×10^{-8}	0.1×10^{-8}

Table 5:

As already explained, the initial problem (5) can be solved with the decomposition into rectangles replaced by a more complex one, made of convex quadrilaterals and quadrilaterals with curved edges to treat the geometry of the initial domain. Since the discretization on these elements is built by using a one-to-one transformation that maps the reference square onto the element, transporting the problem onto the square and approximating the resulting problem on the square (with nonconstant coefficients) by polynomials. So there is no problem in extending the previous results to this geometry.

However, handling fourth-order problems or three-dimensional geometries or nonlinear equations would require further work in order to derive the analogues of estimates (11) to (13). And even in the simplest two-dimensional example, these estimates are not fully optimal.

The mortar element discretization on the new mesh can easily be extended to more complex second-order problems and decompositions into convex quadrilaterals and quadrilaterals with curved edges. Also using the three-dimensional mortar technique as studied in [1], would allow to analyze this discretization in the three-dimensional case.

References

[1] F. Ben Belgacem. Thesis, Université Pierre et Marie Curie, Paris (1993).

[2] C. Bernardi. Indicateurs d'erreur en $h - N$ version des éléments spectraux, *Modél. Math. et Anal. Numér.*

30 (1996), 1-38.

[3] C. Bernardi, M. Dauge, Y. Maday. Polynomials in weighted Sobolev spaces: basics and trace liftings, Internal Report **92039**, Laboratoire d'Analyse Numérique de l'Université Pierre et Marie Curie, Paris (1992).

[4] C. Bernardi, Y. Maday. *Spectral elements*, to appear in the *Handbook of Numerical Analysis*, Vol. V, P.G. Ciarlet and J.-L. Lions eds., North-Holland (1996).

[5] C. Bernardi, Y. Maday. Mesh adaptivity in finite elements by the mortar method, Internal Report **94029**, Laboratoire d'Analyse Numérique de l'Université Pierre et Marie Curie, Paris (1994).

[6] C. Bernardi, Y. Maday, A.T. Patera. A new nonconforming approach to domain decomposition: the mortar element method, *Collège de France Seminar* **XI**, H. Brezis & J.-L. Lions eds., Pitman (1994).

[7] C. Bernardi, Y. Maday, A.T. Patera. Domain decomposition by the mortar element method, in *Asymptotic and Numerical Methods for Partial Differential Equations with Critical Parameters*, H.G. Kaper & M. Garbey eds., N.A.T.O. ASI Series C **384**, Kluwer (1993).

[8] C. Bernardi, B. Métivet, R. Verfürth. Analyse numérique d'indicateurs d'erreur, Internal Report **93025**, Laboratoire d'Analyse Numérique de l'Université Pierre et Marie Curie, Paris (1993).

[9] R. Verfürth. A review of a posteriori error estimation and adaptive mesh-refinement techniques, Internal Report, Institut für Angewandte Mathematik, Universität Zürich (1993).